Indian Journal of Pure & Applied Physics
Vol. 43, January 2005, pp. 51-55

Sol-gel processed TiO_2 films on U-shaped glass-rods as optical humidity sensor

B C Yadav, R K Shukla & L M Bali

Opto-Electronic Research Laboratory, Department of Physics, University of Lucknow, Lucknow 226007

E_mail: balchandra_yadav@rediffmail.com; balchandra_yadav@yahoo.co.in

Received 28 May 2004; revised 4 October 2004; accepted 16 November 2004

The fabrication and characterization of a thick-film optical humidity sensor based on the semiconducting metal-oxide TiO_2 have been described. The sensor element consists of a thin U-shaped borosil glass-rod having different curvature with a film of TiO_2 deposited on it. The films prepared are dried and annealed at 600° C for two hours, which make them rutile, porous and very sensitive to humidity. Both the ends of the U-shaped glass-rods are coupled to optical fibers. Light from a He-Ne laser is launched in to the sensing element through one of them. Light received from the other fibre is fed into an optical power meter. Variations in the intensity of light with changes in humidity from 5% to 95% have been recorded.

[**Keywords:** Humidity sensors, Thick film, Sol-gel process]
IPC Code: G06K 7/10

1 Introduction

The control of humidity is becoming increasingly important for improving quality of life and enhancing industrial process. Humidity sensors based on various working principles have been produced to serve the applications[1]. Humidity sensor in which the sensing element is a thick or thin film have been extensively studied[2-10]. Most of these sensors are based on monitoring changes in the electrical parameters like resistance, conductance or capacitance. Very few reports are available in which optical properties of these films are used to determine the relative humidity[11-18].

The optical humidity sensors investigated in this study consist of a thin U-shaped glass-rod of 1 mm diameter having different curvatures, on which a film of TiO_2 is deposited. Modulations in the intensity of light passing through the glass-rods determine the relative humidity of the environment surrounding it. The refractometer sensor reported by K. Spenner *et al.*[19] has an uncladded U-shaped fibre as its sensing element and is therefore highly fragile. In fact, the U-shaped thin glass rod considered here would be far more sturdy than either the cladded or the uncladded U-shaped optical fibre.

2 U-Shaped Glass Rods

Thin borosilicate glass rods have been bent in the shape of U such that the separation between its two arms is given by $2x$ and the depth of its curvature by y as shown in Fig. 1.

Let the bend ADC of the U-shaped glass rod is the arc of the circle ADCE, as shown in Fig. 2. Also, let the radius of this circle be given by AO = OD = r, the length of the chord AC = 2AB = 2BC, and the depth of curvature BD = r-OB = y. Radius of the bend of the U-shaped rod can then be evaluated from the geometry of Fig. 2. Therefore, from the relation,

$$r^2 = OB^2 + AB^2 = (r-y)^2 + x^2 \quad \ldots (1a)$$

it is found that

$$r = (x^2+y^2)/2y \quad \ldots (1b)$$

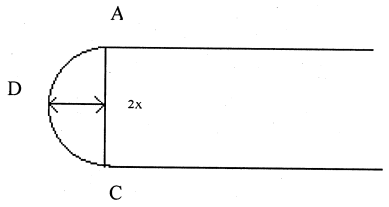

Fig. 1—U-shaped glass rod used for sensing humidity.

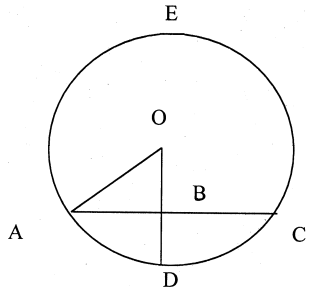

Fig. 2—Bend ADC of the U-shaped glass rod as an arc of the circle ADCE.

The depth of curvature y and the separation $2x$ between the two arms of the five U-shaped glass rods of diameter 1 mm fabricated in the laboratory have the corresponding radius of curvature r which can be evaluated with the help of Eq. (1b). Thus these rods are characterized by the following specifications:

Sensing element *a* :2*x*=6.0 mm, *y*=4.5 mm, *r*=3.3 mm
Sensing element *b* :2*x*=8.0 mm, *y*=4.0 mm, *r*=4.0 mm
Sensing element *c* :2*x*=10.0 mm, *y*=3.5 mm, *r*=5.3 mm
Sensing element *d* :2*x*=12.0 mm, *y*=3.0 mm, *r*=7.5 mm
Sensing element *e* :2*x*=16.0 mm, *y*=2.0 mm, *r*=17.0 mm

Surface morphology of films shown in Figs 3 and 4 of micrographs has been studied. It is found that film on the sensing element *c* (micrograph shown in Fig. 4) is found more porous and uniform.

3 Experimental Details

TheU-shaped thin glass rods of five different radii of curvatures viz. 3.3 mm, 4.0 mm, 5.3 mm, 7.5 mm and 17.0 mm. A film of TiO_2 is deposited on each of these glass-rods by the Sol-gel dip process. The solution in which the thin glass rods are dipped, are prepared by mixing isopropyl titanate and isopropyl alcohol in two ratios i.e. 1:25 [case(i)] and 2:25 [case (ii)] Gel coated films were dried at 100°C for 15 minutes and then annealed at 600°C in air for two hours. Such a treatment makes these films rutile[20-22], porous and therefore sensitive to humidity. They can then be used as sensing elements.

The experimental set-up for the sensor assembly[23-24] is shown in Fig. 5. The U-shaped glass rod, with a TiO_2 film deposited on it, is fixed on the wall of a steel chamber with the help of two holes drilled in it such that the bend remains inside the chamber and the two arms protrude outside. The two ends of these arms are then coupled to plastic optical fibres. Light from an unpolarised 2 mW He-Ne laser source (OSAW, India) or a LED is launched from one of these fibres. Light received from the other fibre is fed into an optical power meter [BenchMark Model, FOPM-101] for measurement of its intensity.

The humidity is increased from 5% to 95% by placing a saturated aqueous solution of potassium sulphate (K_2SO_4) in a small container inside the steel chamber. The relative humidity (RH) is measured by a standard hygrometer (Huger, West Germany). The consequential changes in intensity of light emerging out of the TiO_2 coated U-shaped glass rod, are recorded for each of the thin glass rods. The chamber is then dehumidified upto 10% RH by putting KOH in a dish inside it. It is further dehumidified upto 5% RH by carrying out the heat cleaning cycle of the sensing element. It may be noted that on varying the humidity from 5% to 95% the temperature of the chamber decreases by 4°C . The least count of the hygrometer used here for the measurement of RH is 1% and that of the optical power meter is 0.1 dBm.

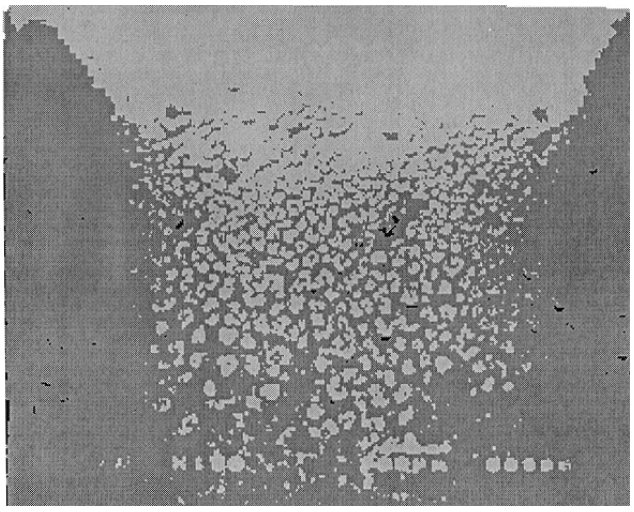

Fig. 3—Scanning micrograph for the ratio 1:25.

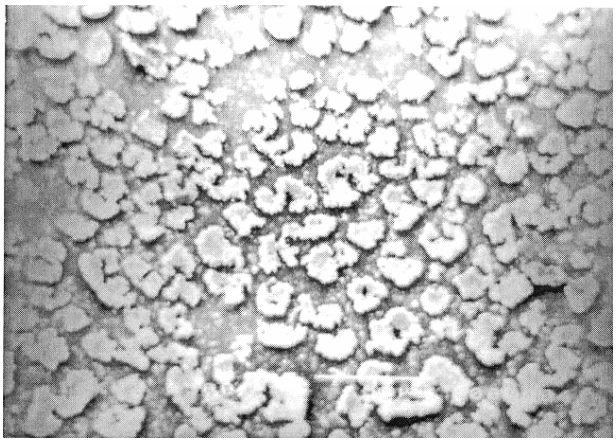

Fig. 4—Scanning micrograph for the ratio 2:25.

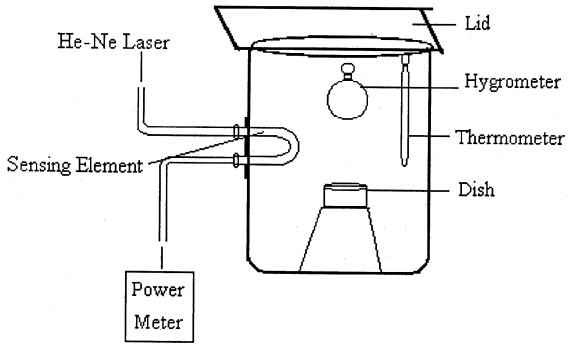

Fig. 5—Experimental set-up.

Observations are taken for the output intensity from one end of the U-shaped sensor, through the coupled plastic fibre, as the humidity inside the chamber is varied. The observations for the different U-shape geometries of these sensors for case (i) are plotted in Fig. 6 and those for case (ii) are plotted in Fig. 7.

For one of the sensing element of case (ii) observations have also been taken using LED (660 nm) as the input light source.

4 Results

4.1 With He-Ne Laser

In this section we present results of the experiments carried out with He-Ne laser as the source of the light. A glance through the graphs plotted for this case in Fig. 6 [case (i)] and Fig. 7 [case (ii)] show that the increase of humidity inside the chamber produces a corresponding decrease in the output intensity. The increase in humidity increases adsorption of water vapours and their condensation in the pores of the TiO_2 film causing an increase in the refractive index of the film interfacing the glass rod. This leads to a greater leakage of light through the sensing element thereby decreasing the output intensity. The sensitivity with which RH can be measured with the help of the U-shaped humidity sensor described above is defined as:

$$S = \Delta I_r / \Delta RH$$

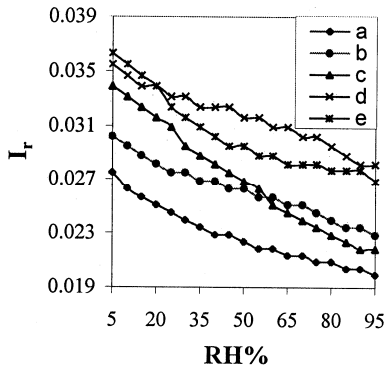

Fig. 6—Variations in the reflected intensity of light I_r against RH% for TiO_2 film deposited on U-shaped glass rods for the ratio 1:25.

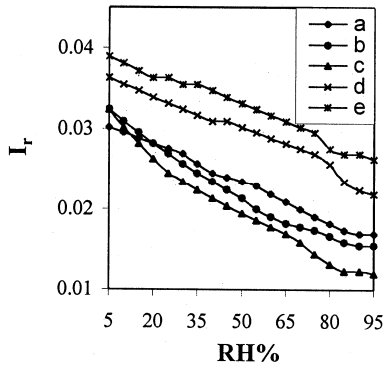

Fig. 7—Variations in the reflected intensity of light I_r against RH% for TiO_2 film deposited on U-shaped glass rods for the ratio 2:25.

4.1.1 Case (i)

Figure 6 shows the corresponding plots for this case. Curves *a, b, c, d* and *e* of correspond to the sensing elements *a, b, c, d* and *e* described in Sec. 2.

It may be seen that the sensing element *a* is sensitive in the lower humidity range of 5%-30%. Its sensitivity is 1.42. But it is less sensitive in the RH range of 30%-60% where its sensitivity is 0.70. Its sensitivity goes down further to 0.58 and 0.47 as RH ranges varying from 60%-85% and 85%-95%, respectively, are approached. Sensing element *b* has the sensitivity 1.06 in the lower range of humidity lying between 5% and 30%, and 0.61 in the middle RH range of 30%-60%, 0.90 and 0.53 are the sensitivities of this sensing element in the higher RH ranges from 60% to 85% and from 85% to 95%, respectively. Sensing element *c* has a reasonably large sensitivity over the entire range of RH from 5% to 85%. Its sensitivities in the RH ranges of 5%-30%, 30%-60% and 60%-85% are 1.75, 1.46 and 1.09, respectively. Sensitivity of this sensing element for its highest RH range from 85% to 95% is only 0.51, which is quite low. Sensing element *d* shows sensitivity of 0.95 in the humidity range of 5%-30% and 0.74 in the middle humidity range of 30%-60%. In the higher humidity ranges from 60% to 85% and from 85% to 95% its sensitivities are 0.82 and 0.66, respectively. The sensing element *e* has a higher sensitivity of 1.88 in the humidity range of 5%-30% and it has a lower sensitivity of 1.15 in the humidity range of 30%-60%. In the next two higher RH ranges of 60%-85% and from 85% to 95% its sensitivities are 0.17 and 0.84, respectively.

4.1.2 Case (ii)

Figure 7 shows the corresponding plots for this case. These plots again show that increase of humidity inside the chamber leads to a decrease in the output power. Curves *a, b, c, d* and *e* correspond to the sensing elements *a, b, c, d* and e respectively. Curve a of Fig. 7 shows sensitivity of 1.32 in the lower humidity range of 5% to 30%, sensitivities of 1.68 and 1.79 in RH ranges 30%-60% and 60%-85%, and the lowest sensitivity of 0.42 in the highest humidity

range of 85%-95%. Sensitivities of sensing element *b* shown by curve b (Fig. 7) are 2.66, 2.22, 1.28 and 0.36 in the RH ranges 5%-30%, 30%-60%, 60%-85% and 85%-95%, respectively. Response of sensing element *c* shown by curve c (Fig. 7) gives the highest sensitivity of 3.57 in the lower RH range of 5%-30% but a lower sensitivity of 1.89 in the middle humidity RH range of 30%-60%. In the higher RH ranges from 60% to 85% and from 85% to 95% sensitivities of this sensing elements are 2.19 and 0.28, respectively. Similarly, the sensitivity of element *d* shown by curve d (Fig. 7) is 1.58 in the RH range of 5%-30% and 1.17 in the middle RH range of 30%-60%. In the higher RH ranges from 60% to 85% and from 85% to 95% its sensitivities are 2.16 and 1.56, respectively. For the sensing element *e* curve e (Fig. 7) shows sensitivity of 1.37 on the RH range of 5%-30%, sensitivity of 1.29 in the RH range of 30%-60%, sensitivity of 1.88 in the higher RH range of 60%-85% and 0.61 in the RH range of 85%-95%.

The study of Figs 6 and 7 shows that the nature of modulation of light emerging out from the U-shaped thin glass rod sensing elements in both the cases (i) and (ii) described above, is similar. When the response of each sensing element for the RH range lying between 5% and 85% is compared for these two cases, the Figs 6 and 7 show that:

(1) Sensing element *a* for case (ii) is more than twice as sensitive as for case (i) in the RH range of 30%-60%, but it is more than three times as sensitive in the RH range of 60% to 85%. (2) Sensing element *b* for case (ii) is more sensitive in the RH ranges of 5%-30% and 60%-85%, but it is more than three times as sensitive in the RH range of 30%-60% as for the case (i). (3) Sensing element *c* for case (ii) is two times more sensitive in the RH ranges of 5%-30% and 60%-85% and only 1.3 times more sensitive in the RH range of 30%-60% as for case (i). (4) Sensing element *d* for case (ii) is more than twice as sensitive in the RH of 60%-85% and only 1.7 times and 1.6 times more sensitive in the RH ranges of 5%-30% and 30%-60% as for the case (i). (5) Sensing element *e* behaving differently, for case (i) is nearly one and a half times as sensitive in the lower RH range of 5%-30% and is less sensitive in all other ranges of RH as for case (ii).

4.2 With LED

The U-shaped optical sensor *c* (curve c, Fig. 7) was found to yield the largest sensitivity. Therefore, the experiment was repeated for the sensing element *c* after replacing the unpolarised He-Ne Laser by U.S.A. made 660 nm Light Emitting Diode as the source of light in the experiment. The experimental set-up for this experiment is the same as that shown in Fig. 5.

The emergent light intensity from the sensing element *c* with varying RH is noted and is plotted against RH% (Fig. 8). The nature of the curve is found to be similar with those obtained using Laser source (Figs 6&7). There is a linear response up to 40% RH, then the curve bends a little and again remains linear up to 95% RH. The sensitivity in the lower humidity range of 5% to 40% is found to be 1.33 and is only 0.03 in the higher humidity range of 40%-95%.

5 Discussion

It is seen that the increase in humidity increases adsorption of water vapour by the porous TiO_2 film causing a corresponding increase in its refractive index. This effectively changes the boundary condition at the cladding-core interface reducing the beam confinement in the guide, thereby reducing the light intensity emerging out through the TiO_2 cladded thin glass rod [Figs 6, 7 and 8]. To start with, the TiO_2 film is free of water molecules and has dry air in its pores. On being exposed to environment of lower humidity, rapid surface adsorption of water vapours into the porous film begins, causing rapid attenuation of the light propagating through the TiO_2 cladded thin glass rod. This attenuation[25] may be attributed to the increased leakage of light into the cladding of the rod the refractive index of which increases as the RH increases. Therefore, the sensitivity is higher in this region. In the higher RH range, the capillary condensation occurs and forms a meniscus in the capillaries of the cladding. The attenuation of light and hence the sensitivity starts decreasing in this

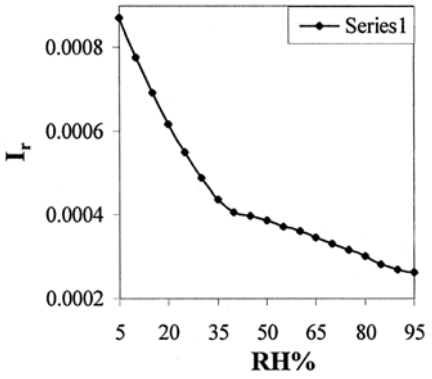

Fig. 8—Variations in the reflected intensity of light I_r against RH% using LED as source for TiO_2 film deposited on U-shaped glass rod for which 2x =10 mm and r =5.3 mm for the ratio 2:25.

range of RH. As the RH increases further the porous TiO_2 film starts becoming saturated resulting in a still smaller sensitivity for this region. Experimental results indicate that above 90% RH changes in the output intensity of light become negligibly small.

Sensing elements for case (ii) are found to show larger sensitivities than those for case (i) because of larger thickness of cladding.

The fast response of the sensors we have observed can be attributed to the fast penetration of water molecules into the cladding. The slow recovery in the response, on the other hand, is caused by a slow desorption process and capillary forces.

The experiments were carried out five times during one year but no aging effect was found and the results obtained earlier were reproduced.

6 Conclusion

Results described above clearly show that the optical humidity sensors can be used with a high degree of sensitivity to measure RH in the broad range of 5%-95%. Reliability and cost-effectiveness characterizes these sensors. Being optical in nature, the sensors investigated here can also be used at unmanned stations.

Acknowledgement

Authors are highly grateful to Dr G.C. Dubey for fruitful discussions and constant encouragement.

References

1 Kulwicki B M, *J.Am.Ceram Soc*, 74 (1991) 697.
2 Wenmin Qu, Jorg-Uwe Meyer,.*Sens Actuators B*, 40 (1997)175.
3 Ansari S G, Karekar R.N. & Aiyer R C, *Proceedings of National Seminar on Physics and Technology of Sensors*, Pune, February 1-3 (1996) C22-1-5.
4 Dubendorter J, *Sens Actuators B*, 38 (1997) 316.
5 Ogwa K, Truchiya S, Kawakami H & Tsutsui T, *Electron Lett*, 15 (1988) 77.
6 Ando M, Kobayashi T & Haruta, *Sens Actuators B*, 32 (1996) 157.
7 Sadaoka Y, SakaiY & Murata Yu-uki, *Sens Actuators B*, 13-14 (1993) 420
8 Sadaoka Y, Sakai Y, Matsuguchi M & Murata Yu-uki, *Sens Actuators B*, 7 (1992) 443.
9 Ibid, *J Electr Sci*, 138 (1991) 614.
10 Ying J, Wan C & He P, *Sens Actuators B*, 62 (2000) 165-170.
11 Narayanaswamy & Wolfbeis, *Optical Sensors* Vol. 1 (Published by Springer, 2004) ISBN 3-540-40888-X.
12 Yadav B C & Shukla R K, *Ind J Pure & Appl Phys*, 41 (2003) 681
13 Weiss M N, Srivastava R & Groger H, *Electr Lett*, 32 (1996) 842.
14 Brook T E, Taib M N & Narayanaswamy R, *Sens Actuators B*, 38 (1997) 272.
15 Muto F B, Fukasawa A & Kamimura M, *Jpn J Appl Phys*, 28 (1989) L 1065.
16 Kharaz A & Jone B E, *Sens Actuators B*, 47 (1995) 491.
17 Ansari Z A, Karekar R N & Aiyer R C, *Thin Solid Films*, 305 (1997) 330.
18 Bariain C, Matias I R, Arregui F J & Lopz-Amo M, *Sens Actuators B*, 69 (2000) 127.
19 Spenner K, Singh M D, Schulte H & Boehnel H J, *SPIE Milestone Ser*, 108 424-426.
20 Tang H, Prasad K, Sanjines R, *et al*. *J Appl Phys*, 75 (1994).
21 Wen T, Gao J, Shen J & Zhow Z, *J Mat Sci*, 36 (2001) 5923.
22 Jiaguo yu, Jimmy C yu & Xiujian Zhao Zz, *J Sol-Gel Sci & Technol*, 24 (2002) 9.
23 Bali L M, Dubey G C, Yadav B C, Shukla R K, *7th National Seminar on Physics and Technology of Sensors, Pune,India held during Feb. 14-16 (2000)*. p. C.35.1-C.35.6.
24 Shukla S K, Parashar G K, Mishra A P, Mishra,Puneet, Yadav B C, Shukla R K, Bali L M & Dubey G C *Sensors and Actuators B*, 98(2004) 5.
25 Kumar A, Shenoy M R, Pal B P & Goyal I C, *J Inst Telecommun Eng*, 32 (1986) 347.